Mössbauer Spectroscopy of Iron Biomineralization Products in Magnetotactic Bacteria

RICHARD B. FRANKEL, GEORGIA C. PAPAEFTHYMIOU, and RICHARD P. BLAKEMORE

1. Introduction to Mössbauer Spectroscopy

Mössbauer spectroscopy is a nuclear γ-ray resonance technique that has been extensively applied to the study of the electronic properties of iron in biological systems. The power of the technique lies in its sensitivity to the effects of the physical environment (nature and disposition of ligands, magnetic structure, etc.) on ^{57}Fe nuclei. Moreover, it is sensitive only to ^{57}Fe so it is not affected by other elements in the system, except as they affect the environment of the iron atoms. The technique allows discrimination of nonequivalent iron sites as opposed to magnetic susceptibility or magnetization measurements which lump together contributions from all the sources in the sample. As extensive reviews of Mössbauer spectroscopy are available (Greenwood and Gibb, 1971; Bancroft, 1973; Cohen, 1976, 1981) we will only give a brief introduction here, focusing on ^{57}Fe. This will be followed by a review of spectroscopy of iron in biomineralization products, and of magnetic inclusions in magnetotactic bacteria.

1.1. Nuclear γ-Ray Absorption

Nuclei have discrete energy levels that correspond to different configurations of the constituent protons and neutrons. Each energy level is characterized by a spin angular

RICHARD B. FRANKEL and GEORGIA C. PAPAEFTHYMIOU • Francis Bitter National Magnet Laboratory, Massachusetts Institute of Technology, Cambridge, Massachusetts 02139. RICHARD P. BLAKEMORE • Department of Microbiology, University of New Hampshire, Durham, New Hampshire 03824.

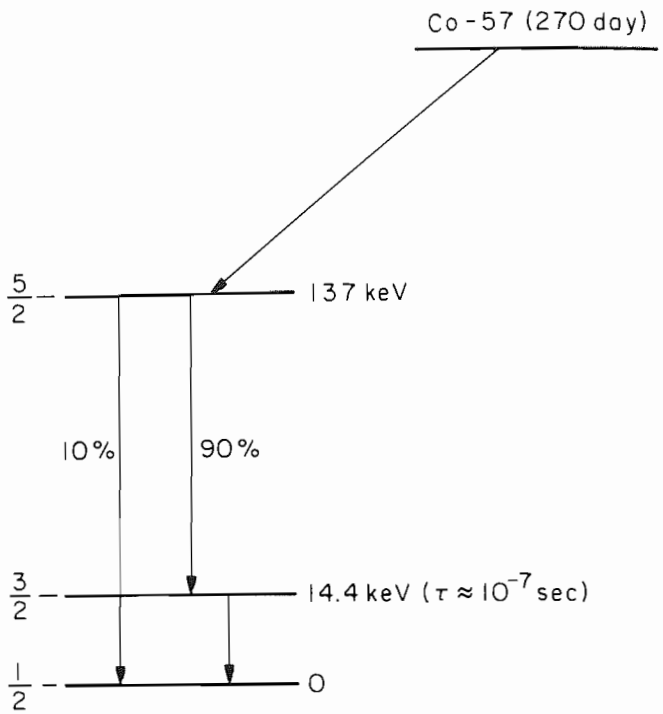

Figure 1. Decay scheme of ^{57}Co to ^{57}Fe.

momentum and other physical parameters. The low-lying energy levels of 2.2% abundant ^{57}Fe are shown in Fig. 1. The stable ground state has a spin $I_0 = \frac{1}{2}$ and there is an excited state at $\Delta E = 14.4$ keV with spin $I_{14.4} = \frac{3}{2}$. An ^{57}Fe nucleus in the excited state, for example, following the decay of radioactive ^{57}Co, can decay to the ground state by emitting a 14.4-keV γ ray (or by the alternative process of electron conversion), with a half-life of $\sim 10^{-7}$ sec. Conversely, a nucleus in the ground state can be excited to the 14.4-keV state by absorption of a γ ray with energy $E_\gamma = 14.4$ keV. The absorption probability or cross section is a function of γ-ray energy. It is a maximum at ΔE and falls to one-half its maximum value when $E_\gamma = \Delta E \pm \Gamma/2$, where Γ is the intrinsic linewidth of the 14.4-keV excited state. The width is related to the lifetime of the state by the uncertainty principle:

$$\Gamma = h/2\pi\tau \tag{1}$$

where h is Planck's constant. Because $\tau = 10^{-7}$ sec, $\Gamma = 5 \times 10^{-9}$ eV for the 14.4-keV state. Thus, $\Gamma/\Delta E \simeq 10^{-12}$!

Because electromagnetic radiation has momentum, the nucleus must recoil when it absorbs the γ ray in order to conserve linear momentum. Thus, some of the γ-ray energy goes into recoil energy and is not available for excitation. The momentum of the γ ray $p = E_\gamma/c$, hence the recoil energy

$$R = p^2/2M_n = E_\gamma^2/2M_nc^2 \tag{2}$$

where M_n is the mass of the nucleus and c is the speed of light. For ^{57}Fe, $R \simeq 0.002$ eV, i.e., $R \gg \Gamma$. Because of nuclear recoil, the cross section for absorption will be low even when E_γ is precisely equal to ΔE. Mössbauer's great discovery was that if the nucleus is

embedded in a solid, there is a certain probability that the recoil momentum will be taken up by the solid as a whole. In those cases, $R \rightarrow 0$ because M_n in the denominator of Eq. (2) is replaced by the mass of the entire solid, i.e., of the order of 10^{23} times the mass of the single nucleus. Hence, the Mössbauer effect is recoilless nuclear γ-ray resonance.

The probability of recoilless absorption f is a function of M_n, E_γ, and the vibrational characteristics of the solid. It is temperature dependent, decreasing with increasing temperature. These and various other considerations limit the number of isotopes in addition to ^{57}Fe for which resonant absorption can be observed.

The most convenient source of 14.4-keV γ rays for Mössbauer spectroscopy of iron in a particular material is radioactive ^{57}Co which decays to ^{57}Fe with a half-life of 270 days. As in the case of γ-ray absorption, γ-ray emission also involves recoil momentum, but if the radioactive nuclei are embedded in a solid, recoilless emission can occur. In practice, ^{57}Co, which is produced in a cyclotron, is usually electroplated and diffused into a metallic host such as Cr, Cu, Rh, Pd, or Pt.

In order to observe the resonance, it is necessary to vary the γ-ray energy by an amount of the order of several times Γ. This is accomplished by changing the effective frequency of the γ ray through the Doppler effect by moving the source of γ rays relative to the absorber. The change in energy

$$\delta E = (v/c)E_\gamma \tag{3}$$

where v is the relative velocity. For ^{57}Fe, $\delta E = 2\Gamma$ when $v = 0.2$ mm/sec so velocities of the order of 1 mm/sec to 1 cm/sec are sufficient to sweep out the entire line.

The spectrum is most often observed by measuring the intensity of γ rays transmitted through the absorbber as a function of relative velocity which is equivalent to energy [Eq. (3)]. At high positive or negative velocities, high transmission occurs because the γ rays have been Doppler shifted off resonance. At velocities close to zero, the absorption cross section is high and the transmitted intensity is relatively low. The experimental linewidth is at least 2Γ because it includes the intrinsic widths of both the source and the absorber.

1.2. Hyperfine Interactions

The usefulness of Mössbauer spectroscopy for the study of iron in materials stems from the fact that interactions of the nucleus with the environment perturb the nuclear levels with consequent changes in the γ-ray absorption spectrum (Freeman and Frankel, 1967). These interactions are collectively known as hyperfine interactions because they result in energy shifts or splittings of the nuclear levels which are tiny compared to 14.4 keV but which are nevertheless comparable or larger than Γ.

The three most important interactions leading to spectral features include (1) the isomer shift, (2) the quadrupole splitting, and (3) the magnetic hyperfine splitting (Fig. 2). In general, these interactions result in nuclear-level energy changes or splittings and can be written as a product of nuclear and electronic factors. The nuclear factors are measured properties associated with each nuclear level. The electronic factors depend on electronic environment. Determination of the electronic factors gives information about the electron structure in the solid.

The isomer shift arises from the fact that the ground state and the 14.4-keV excited state have different mean-squared charge radii. Hence, the electrostatic interaction between the nuclear charge and the atomic electrons will be different for ground and excited states and the energy difference between the two states will be affected by the total electronic charge density at the nucleus. This charge density is mostly due to the atomic s electrons and is affected by the chemical environment. Thus, the splitting between ground and

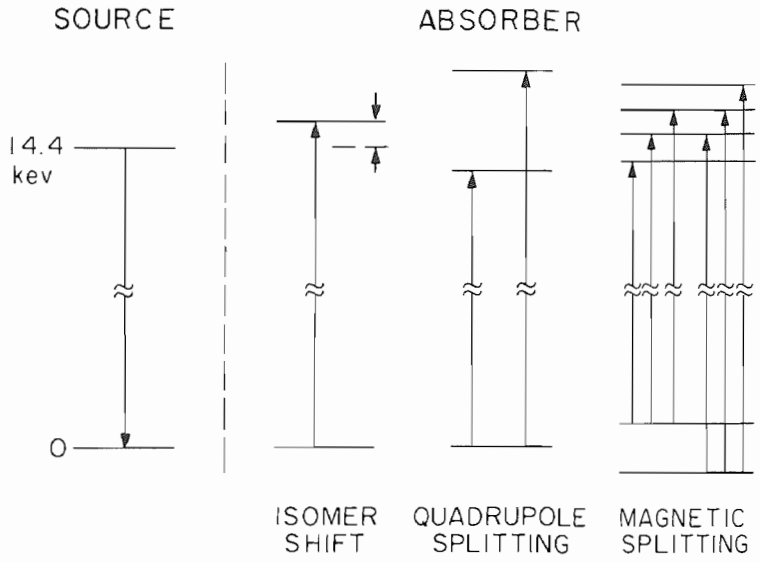

Figure 2. Effect of hyperfine interactions on the ^{57}Fe nucleus.

excited nuclear states will be different in different chemical environments, resulting in a relative shift of the centroid of the absorption line. If the γ-ray source is chemically different than the absorber, the absorption line will no longer be centered at $v = 0$, but will be shifted to higher or lower velocities. Large differences in the s-electron density and consequently large isomer shifts occur for iron atoms in different oxidation states. The shift between Fe^{2+} and Fe^{3+} can be more than 1 mm/sec. Isomer shifts are generally quoted relative to iron metal.

A splitting of the 14.4-keV nuclear levels can result from the interaction of the nuclear quadrupole moment with an electric field gradient due to the electrons if the local symmetry about the iron atom is less than cubic. As the 14.4-keV state has spin $I = \frac{3}{2}$, it is $2I + 1$ = fourfold degenerate. The quadrupole interaction splits the states into two sublevels, each with twofold degeneracy. This results in an absorption spectrum with two lines of equal intensity (for a polycrystalline absorber). The magnitude of the splitting ΔE_Q is a direct measure of the electric field gradient which depends on the local electronic environment and the orbital angular momentum. Fe^{3+} (high spin) has a half-filled $3d$ shell and no orbital angular momentum and the quadrupole splittings are typically small, $\Delta E_Q < 1.0$ mm/sec. Fe^{2+} can have unquenched orbital angular momentum and consequently large quadrupole splittings, $\Delta E_Q > 2.0$ mm/sec, because of the extra electron outside of the half-filled shell.

A magnetic field acting on the nucleus completely raises the fourfold degeneracy of the $I = \frac{3}{2}$ excited state and the twofold degeneracy of the $I = \frac{1}{2}$ ground state. The splitting between the nuclear sublevels depends on the magnitude of the magnetic field at the nucleus and the magnetic moments of the ground and excited nuclear states. Although there are eight possible combinations of the four excited sublevels with the two ground sublevels, only six transitions are allowed and hence only six lines are usually observed in the Mössbauer spectrum (Fig. 3). An effective magnetic field at the nucleus, the magnetic hyperfine field H_{hf}, results from the interaction of the nuclear magnetic moment with the atomic magnetic moment. In high-spin Fe^{3+} with five unpaired electrons, the magnitude of H_{hf} is typically of the order of 500 kOe and negative in sign, that is, the effective field due to the magnetic hyperfine interaction is oriented antiparallel to the atomic magnetic

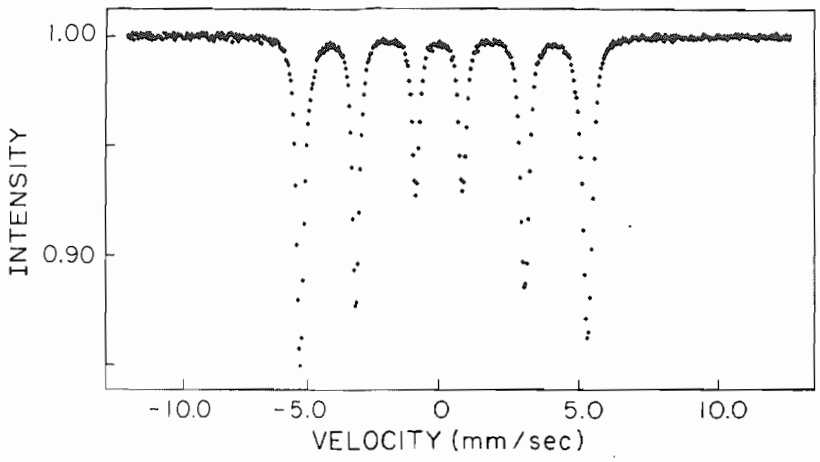

Figure 3. Mössbauer spectrum of iron metal at room temperature.

moment. In Fe^{2+} the atomic moments are typically smaller and more variable from compound to compound because of orbital contributions; this is reflected in smaller and more variable magnetic hyperfine fields. In iron metal where the moment per iron atom is 2.2 μ_B, the magnetic hyperfine field is –330 kOe (at room temperature).

The magnetic field causes the nucleus to precess with a frequency ν_L that is proportional to the field strength; the time for a single complete precession is known as the Larmor precession time. For an Fe^{3+} atom with $|H_{hf}| = 500$ kOe, this is about 10^{-7} sec. If the field fluctuates or changes sign due to relaxation of the atomic moment on a time scale less than the Larmor precession time, the magnetic splitting will not be observed and the Mössbauer spectrum will consist of a single line (or quadrupole doublet). This is generally the case for paramagnetic iron atoms. In ferro-, ferri-, or antiferromagnetic iron compounds where each atomic moment is oriented in a fixed crystallographic direction, the full magnetic splitting is observed in the spectrum. As the temperature increases through the Néel or Curie point (the magnetic ordering temperature) above which the material is paramagnetic, the spectrum splitting decreases and collapses to a single line (or quadrupole doublet), reflecting the transition from magnetic order to paramagnetism.

The magnetic splitting can also be observed in paramagnets when the electron spin is polarized by an external magnetic field. The magnetic hyperfine splitting depends on degree of polarization or magnetization of a paramagnet, which varies with H_0/T up to its full or saturation value. However, in an external field, two additional factors come into play. First, the field at the nucleus H_n is now the vector sum of the applied field H_0 and the magnetic hyperfine field H_{hf}:

$$\mathbf{H}_n = \mathbf{H}_{hf} + \mathbf{H}_0 \qquad [4]$$

In paramagnets where the atomic moment is polarized parallel to H_0, the equation reduces to a scalar equation and H_0 adds or subtracts from H_{hf}. Because H_{hf} is usually negative, the net field is the difference between H_{hf} and H_0. For example, Fe^{3+} with $|H_{hf}| = 500$ kOe in a 60-kOe external field at low temperature would have a spectral splitting corresponding to 440 kOe. Second, the relative intensities of the spectral lines depend on the orientation of H_n with respect to the γ-ray propagation direction. If the γ rays are propagated parallel to the field direction, the relative intensities of the six lines are 3:0:1:1:0:3. If the γ rays are propagated perpendicular to the field direction, the relative intensities are

3:4:1:1:4:3. In a polycrystalline, magnetically ordered material, the relative intensities average to 3:2:1:1:2:3.

If a magnetically ordered material is placed in an external magnetic field, similar effects occur (Chappert *et al.*, 1979). In a ferromagnet, the magnetization is generally polarized parallel to H_0, in which case the field at the nucleus is the difference between H_{hf} and H_0. The spectral intensities follow the same rules as outlined above. In a ferrimagnet, where there are two or more magnetic sublattices with antiparallel moment orientation, the net moment of the material will orient parallel to the applied field and the field will subtract from the hyperfine field of those atoms whose moments are oriented parallel to the net moment, but will add to the hyperfine fields of those atoms whose moments are oriented antiparallel to the net moment. In antiferromagnets, the moments of the two antiparallel sublattices cancel each other and there is no net moment to orient in the applied field. The applied field simply broadens the lines without changing their positions or relative intensities compared with zero field.

Superparamagnetism in small particles of magnetically ordered materials can be observed in the Mössbauer spectrum. In this phenomenon, thermal energy excites transitions of the magnetization, or of the sublattice magnetizations in antiferromagnets, between energetically equivalent crystallographic axes. These transitions are opposed by energy barriers proportional to KV, where K is the anisotropy energy per unit volume and V is the volume of the particle. K is a constant, characteristic of each magnetic material. The frequency of transition is given by

$$f = f_0 \exp(-KV/2k_BT) \tag{5}$$

where f_0 is a constant and k_B is Boltzmann's constant. Changes in the Mössbauer spectrum occur when $f \simeq \nu_L$, the Larmor precession frequency, as discussed above for paramagnets. For Fe^{3+} with a hyperfine field of 500 kOe, $\nu_L \simeq 10^7$ sec^{-1}. According to Eq. (5), this condition will occur at a temperature T_B for a given particle size. For $T < T_B$, one will observe the full magnetic splitting in the spectrum. For $T > T_B$, one will observe a collapsed or paramagnetic spectrum, i.e., a single line or quadrupole doublet. If there is a distribution of particle sizes in the sample, the condition $f = \nu_L$ will be satisfied in different particles at different temperatures. Thus, there will be a region of temperature over which the six-line spectrum and the collapsed spectrum coexist, with the latter increasing in intensity and the former decreasing in intensity with increasing temperature. This is illustrated in the case of the iron storage protein ferritin discussed below. Note that the condition for observation of superparamagnetism by the Mössbauer effect is different than that for magnetization measurements. If $f = 1$ sec^{-1}, the remanent magnetization will decay rapidly but the particle will be stable on the Mössbauer time scale.

1.3. Spectroscopy of Iron Oxides and Hydroxides

Iron in a large number of compounds and minerals has been studied by Mössbauer spectroscopy. Iron oxides and hydroxides are particularly relevant to iron biomineralization processes so we will briefly review their spectral features here.

α-Fe_2O_3, hematite, has a close-packed oxygen lattice with Fe^{3+} ions in octahedral sites. The magnetic ordering temperature is 950°K. Up to about 250°K, the magnetic ordering is antiferromagnetic. At 250°K, the material undergoes a transition known as the Morin transition to a weakly ferromagnetic state in which the two sublattices cant toward each other producing a small net moment. The Mössbauer spectrum is a single six-line pattern with a magnetic splitting of 515 kOe at room temperature (Fig. 4) and 540 kOe at

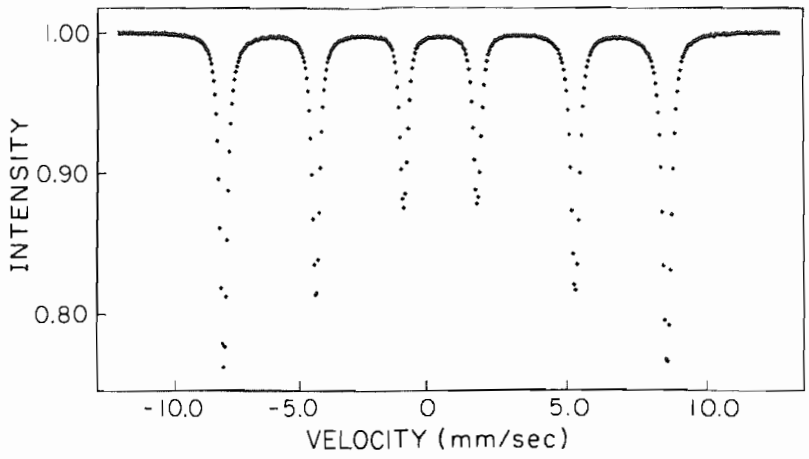

Figure 4. Mössbauer spectrum of α-Fe_2O_3 at room temperature.

4.2°K. The spectrum undergoes subtle changes at the Morin transition (van der Woude, 1966).

γ-Fe_2O_3, maghemite, has a spinel (xy_2O_4) structure in which Fe^{3+} ions in the x sites are tetrahedrally coordinated and Fe^{3+} ions in the y sites are octahedrally coordinated. Antiparallel alignment of iron atoms in x and y sites results in a ferrimagnetic structure. The Mössbauer spectra of iron in the two sites are almost identical but they can be distinguished in an external magnetic field. The hyperfine fields are about 490 and 500 kOe for the x and y sites, respectively, at room temperature (Armstrong *et al.*, 1966).

Fe_3O_4, magnetite, has an inverse spinel structure (xy_2O_4) in which x is Fe^{3+} in tetrahedrally coordinated sites and the two y's are Fe^{2+} and Fe^{3+} in octahedrally coordinated sites. The magnetic structure is ferrimagnetic with the Fe^{2+} and Fe^{3+} in octahedral sites aligned parallel to each other and antiparallel to Fe^{3+} in tetrahedral sites. At room temperature, there are rapid electron transitions between iron atoms in the y sites and the Mössbauer spectrum consists of two overlapping subspectra, one due to Fe^{3+} in x sites, the other an averaged spectrum due to Fe^{2+} and Fe^{3+} in y sites (Fig. 5a). The latter spectrum has a smaller hyperfine splitting (H_{hf} = 453 kOe) and a positive isomer shift compared to the x-site spectrum (H_{hf} = 491 kOe), reflecting the ferrous character of the y sites. Below about 120°K, the temperatures of the so-called Verwey transition, Fe_3O_4 has a complex magnetic structure which results in two partially resolved subspectra, one with H_{hf} = 500 kOe, the other with H_{hf} = 480 kOe (Fig. 5b). The former is due to Fe^{3+} in x and in y sites, which, like γ-Fe_2O_3, have similar spectra. The latter subspectrum is due to Fe^{2+} in y sites (Banerjee *et al.*, 1967; Hargrove and Kundig, 1970).

Mössbauer studies of small particles of Fe_3O_4 have also been carried out, with observation of superparamagnetic effects (McNabb *et al.*, 1968).

α-FeOOH, geothite, has Fe^{3+} atoms in distorted octahedral sites. The structure is antiferromagnetic below about 400°K. The magnetic splitting of the Mössbauer spectrum at low temperature is about 500 kOe, which decreases to 380 at room temperature (Forsyth *et al.*, 1968). β-FeOOH also has Fe^{3+} in octahedral sites, but the structure is nonstoichiometric. The magnetic ordering is antiferromagnetic below 295°K and the magnetic splitting of the Mössbauer spectrum is 475 kOe at low temperature (Dezsi *et al.*, 1967). γ-FeOOH, lepidocrocite, is similar to β-FeOOH, but with a complex layer structure. It is paramagnetic to below 77°K where it becomes antiferromagnetically ordered. However, the Néel temperature is not well defined and magnetically split and collapsed spectra coexist over about

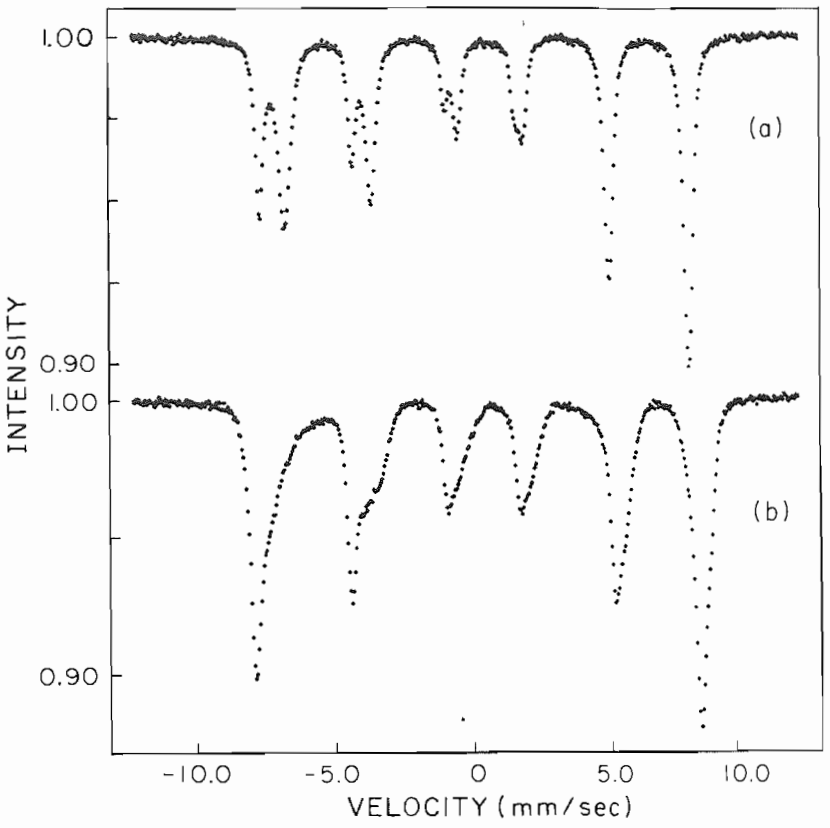

Figure 5. Mössbauer spectrum of Fe_3O_4 at (a) room temperature and (b) 80°K.

10°K. The low-temperature magnetic hyperfine field is 460 kOe (Johnson, 1969). δ-FeOOH has Fe^{3+} atoms in a hexagonally close-packed oxygen lattice with unequal numbers of Fe^{3+} ions in different layers. Unlike the other FeOOH structures, the magnetic structure is ferrimagnetic with two overlapping Mössbauer subspectra at 80°K with magnetic hyperfine fields of 505 and 525 kOe (Dezsi *et al.*, 1967).

$5Fe_2O_3 \cdot 9H_2O$, ferrihydrite, is a naturally occurring hydrous iron oxide which is thought to be similar to the iron core of the iron storage protein ferritin. Natural and synthetic samples exhibit varying degrees of crystallinity and corresponding variations in X-ray diffraction patterns. It contains Fe^{3+} ions in octahedral sites, coordinated to O, OH, and OH_2. The Mössbauer spectrum at room temperature consists of a quadrupole doublet with broad lines, indicating several slightly inequivalent iron sites. At 4.2°K, a magnetically split spectrum with $H_{hf} \simeq 500$ kOe is obtained, but again with broad lines indicating a distribution of magnetic hyperfine fields (Murad and Schwertmann, 1980).

Spectra for a naturally occurring amorphous iron oxide gel have also been obtained. This material has a composition corresponding to $Fe(OH)_3 \cdot 0.9H_2O$ with octahedrally coordinated iron atoms but no long-range structural order. For $T > 20$°K, the spectrum consists of a quadrupole doublet. At 4.2°K, the spectrum is split with a hyperfine field $H_{hf} \simeq$ 460 kOe. External field measurements indicate that the material is paramagnetic for $T >$ 100°K, superparamagnetic for 10°K $< T <$ 100°K, and magnetically ordered below 10°K (Coey and Readman, 1973).

TABLE I. Mössbauer Parameters at 80°K

Material	δ (mm/sec)[a]	ΔE_Q (mm/sec)[b]
A. magnetotacticum		
Spectrum B	0.47 ± 0.03	0.65 ± 0.05
Spectrum C	1.32	3.17
Nonmagnetic cells	0.47	0.68
Cloned, nonmagnetic cells	0.51	0.65
Ferritin	0.47	0.73
E. coli		
Storage material	0.50	0.66
Molpadia intermedia		
Dermal granules	0.48	0.84
Ferrihydrite[c]	0.47	0.74
Amorphous ferric gel[d]	0.47	0.81

[a] Isomer shift relative to iron metal at room temperature.
[b] Quadrupole splitting.
[c] Murad and Schwertmann (1980).
[d] Coey and Readman (1973).

1.4. Biomineralization Products

A number of iron biomineralization products have been studied by Mössbauer spectroscopy (Table I). An important class of iron biominerals occur in the cores of the iron storage proteins including ferritin, hemosiderin, and gastroferrin. These proteins are large spherical molecules, 120 Å in diameter with 70-Å-diameter iron-containing cores. The iron is sequestered as a ferric oxyhydroxide of approximate composition $(FeOOH)_8 \cdot FeO \cdot PO_4H_2$ (Blaise *et al.*, 1965).

The Mössbauer spectrum of horse spleen ferritin shows evidence of superparamagnetism for 20°K < T < 60°K. Below 20°K, the spectrum is magnetically split with $H_{hf} \simeq 500$ kOe. Above 60°K, the spectrum is a quadrupole doublet. Between 20 and 60 kOe, the magnetically split spectrum and the quadrupole doublet coexist with the intensities of the former and latter respectively decreasing and increasing with increasing temperature. The spectral effects in this temperature range are consistent with an average particle diameter of 70 Å and an anisotropy constant of $\sim 10^4$ ergs/cm^3. Hemosiderin gives spectra that are very similar to those of ferritin (Fig. 6). The spectra of ferritin from the fungus *Phycomyces* and of bacterioferritin from *Azotobacter* are similar to mammalian ferritin except that the superparamagnetic behavior is observed over lower temperature ranges. If the core compositions in all ferritins are similar, we can assume that the decrease in the blocking temperatures reflect smaller particle sizes in the plant and bacterioferritins (Oosterhuis and Spartalian, 1976).

An iron-rich storage material of as yet unknown composition has been found in *E. coli* and other prokaryotes, *P. mirabilis* and *M. capricolum*. The Mössbauer spectrum for T > 10°K of the iron storage materials from *E. coli* is a quadrupole doublet with parameters characteristic of high-spin Fe^{3+}. A six-line magnetic hyperfine spectrum with an effective magnetic field at the nucleus of 430 kOe is observed at T < 1°K. Above 1°K, the lines broaden and the splitting decreases with increasing T and collapses into the quadrupole doublet at about 3.5°K. Between 1.2 and 3.5°K, the doublet and sextet are superposed, indicating a spread of magnetic transition temperatures. This indicates lower-energy magnetic interactions between iron atoms than in ferritin, perhaps reflecting less dense packing of the iron atoms than in ferritin (Bauminger *et al.*, 1980).

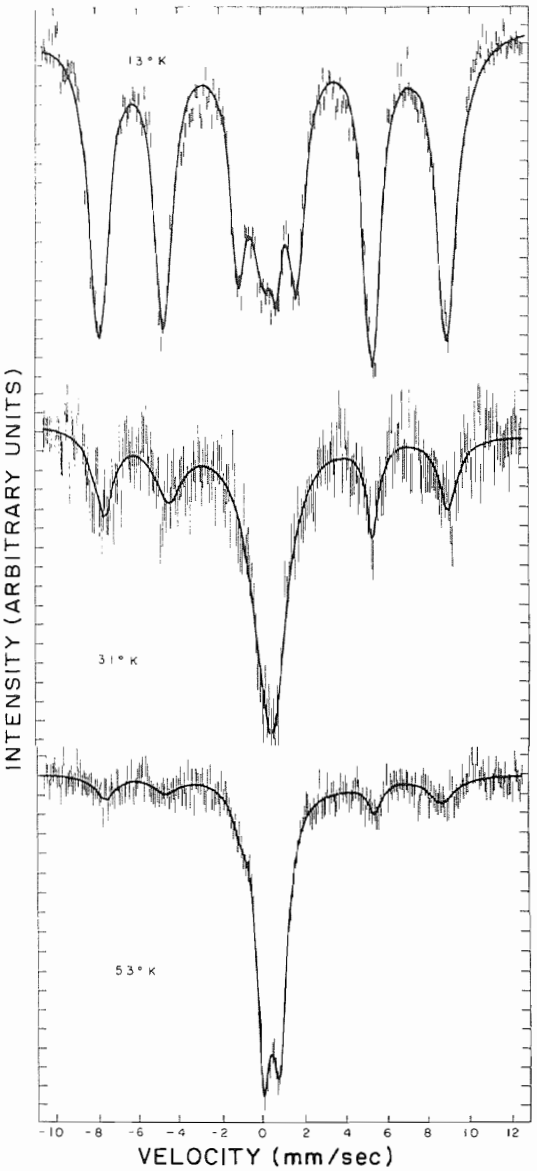

Figure 6. Mössbauer spectra of hemosiderin in heart tissue. From Kaufman *et al.* (1980).

Molpadia intermedia is a species of marine invertebrate that synthesizes iron- and phosphate-rich dermal granules ranging in size from 10 to 350 μm. These serve as strengthening agents in the connective tissues of their dermis. The granules consist of layers composed of two types of spherical to ellipsoidal subunits 0.03 to 0.24 μm in diameter, separated and alternately encapsulated by organic material. One type of subunit contains water, iron, and phosphate with lesser amounts of calcium and magnesium. These deposits are X-ray amorphous and in turn consist of electron-dense subunits 90–140 Å in diameter. The iron is present in the form of hydrous ferric polymeric units similar to the iron-containing micelles of ferritin (Lowenstam and Rossman, 1975).

The Mössbauer spectrum at temperatures between 10 and 300°K is a broadened quadrupole doublet indicating a distribution of electric field gradients at the iron sites. Below

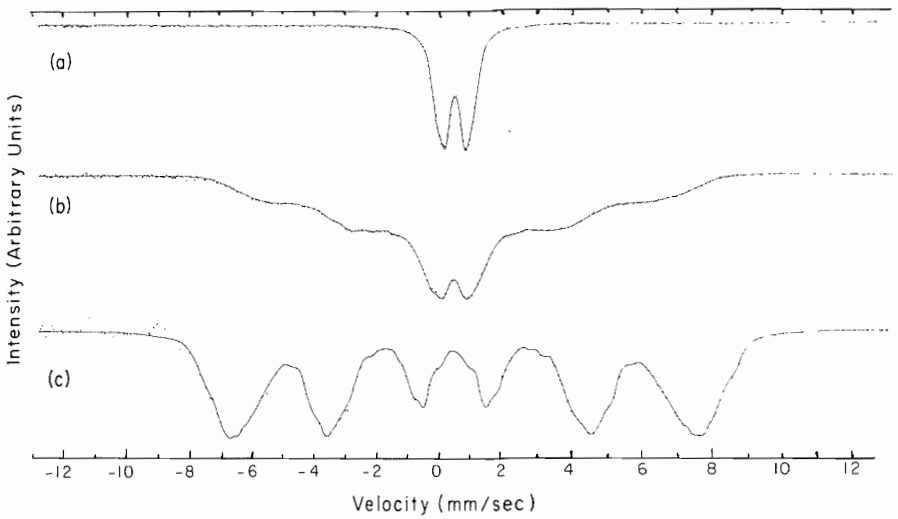

Figure 7. Mössbauer spectra of iron phosphatic dermal granules from *Molpadia intermedia* at (a) 20, (b) 7.2, and (c) 1.6°K. From Ofer *et al.* (1981).

10°K, the spectrum broadens and magnetic hyperfine structure appears, with the effective magnetic field at the nucleus increasing with decreasing temperature. The breadth of the lines indicates a distribution of magnetic hyperfine fields. At 1.6°K, the mode of the distribution is at 420 kOe and moves to progressively lower fields with increasing T, collapsing at about 10°K (Fig. 7). The quadrupole doublet and the magnetically split spectra coexist from ~ 8.0 to 10.0°K. The collapse of the magnetic hyperfine spectrum is indicative of a magnetic transition at about 10°K. A longitudinal magnetic field of 80 kOe at 4.2°K broadens the lines without substantially changing the line positions or relative intensities. This indicates antiferromagnetic ordering of the iron atoms in the granules (Ofer *et al.*, 1981).

2. Application of Mössbauer Spectroscopy to Magnetotactic Bacteria

2.1. Magnetotaxis in Bacteria

Magnetotactic bacteria are various species of aquatic microorganisms that orient and swim along magnetic field lines (Blakemore, 1975, 1982; Moench and Konetzka, 1978; Blakemore and Frankel, 1981). All magnetotactic cells examined to date by electron microscopy contain iron-rich, electron-opaque particles (Balkwill *et al.*, 1980; Towe and Moench, 1981). In several species of magnetotactic bacteria, and possibly all, the particles consist of magnetite, Fe_3O_4 (Frankel *et al.*, 1979). Cuboidal, rectangular, parallelepiped, and arrowhead-shaped particles occur in different species with typical dimensions of 400 to 1200 Å. This places the Fe_3O_4 particles in the single-magnetic-domain size range. In most species, the particles are arranged in chains, which impart a magnetic moment to the cell, parallel to the axis of motility. The moment is sufficiently large that the bacterium is oriented in the geomagnetic field at room temperature as it swims, i.e., the chain of Fe_3O_4 particles functions as a biomagnetic compass (Frankel and Blakemore, 1980). The organism thus propels itself along the geomagnetic field lines. The direction of migration

depends on the orientation of the biomagnetic compass. Those with north-seeking pole forward migrate north along the field lines. Those with south-seeking pole forward migrate south. It has been found that north-seeking bacteria predominate in the northern hemisphere while south-seeking bacteria predominate in the southern hemisphere (Blakemore *et al.*, 1981; Kirschvink, 1980). The vertical component of the inclined geomagnetic field selects the predominant polarity in each hemisphere by favoring those cells whose polarity causes them to be directed downward toward the sediments and away from the toxic effects of the oxygen-rich surface waters. At the geomagnetic equator where the vertical component is zero, both polarities coexist; presumably, horizontally directed motion is equally beneficial to both polarities in reducing harmful upward migration (Frankel *et al.*, 1981; Frankel, 1982).

In the freshwater magnetotactic spirillum, *Aquaspirillum magnetotacticum*, iron comprises 2% or more of the cellular dry weight. Electron microscopic studies of this organism show that the Fe_3O_4 particles are cuboidal, 400–500 Å in width, and are arranged in a chain that longitudinally traverses the cell (Fig. 8). The particles are enveloped by electron-transparent and electron-dense layers; a particle and its enveloping membrane has been termed a magnetosome (Balkwill *et al.*, 1980).

Because *A. magnetotacticum* is cultured in a chemically defined medium in which iron is available as soluble ferric quinate (Blakemore *et al.*, 1979), the presence of intracellular Fe_3O_4 implies a process of bacterial precipitation of this mineral, with control of particle size, number, and location in the cell.

In order to elucidate the Fe_3O_4 biomineralization process, we have studied cells and cell fractions, some isotopically enriched in ^{57}Fe, by Mössbauer spectroscopy. Cells of a nonmagnetotactic variant that accumulated iron but did not make Fe_3O_4 and of a cloned, nonmagnetotactic strain that accumulated less iron, were also studied. The results suggest that Fe_3O_4 is precipitated by reduction of a hydrous iron oxide precursor (Frankel *et al.*, 1983).

2.2. Mössbauer Spectroscopy

Mössbauer spectra of wet packed cells enriched in ^{57}Fe at 200°K and at 80°K are shown in Figs. 9 and 10, respectively. The 200°K spectrum can be analyzed as a superposition of spectra corresponding to Fe_3O_4 (spectrum A), a broadened quadrupole doublet with parameters characteristic of ferric iron (spectrum B), and a weak quadrupole doublet with parameters corresponding to ferrous iron (spectrum C) (Table I). Spectrum A is itself a superposition of subspectra corresponding to the Fe^{2+} and Fe^{3+} in octahedral sites (A_2) and the Fe^{3+} in tetrahedral sites in Fe_3O_4 (A_1).

Spectrum B is also observed in lyophilized cells and has isomer shift and quadrupole splitting parameters similar to iron in ferritin and in the mineral ferrihydrite, indicative of ferric iron with oxygen coordination. The relative intensity of B to A is somewhat variable from sample to sample, depending on growth conditions. At 80°K, spectrum A corresponds to Fe_3O_4 below the Verwey transition (Fig. 5) and the parameters of spectrum B and the relative intensity of B to A are relatively unchanged compared to the spectrum at 250°K. Between 80 and 4.2°K, however, the intensity of B decreases with decreasing temperature so that at 4.2°K, only a residual doublet remains. A similar temperature dependence for spectrum B is also obtained in lyophilized cells.

The isomer shift and quadrupole splitting parameters of spectrum C correspond to high-spin ferrous iron in coordination with oxygen or nitrogen. This spectrum was not observed with lyophilized cells, possibly as a result of oxidation during sample preparation. Wet packed cells kept unfrozen under anaerobic conditions contain increased amounts of material responsible for spectrum C and correspondingly less material with

Figure 8. Electron micrograph of magnetosomes in *A. magnetotacticum*. The bacterium is approximately 3 μm long.

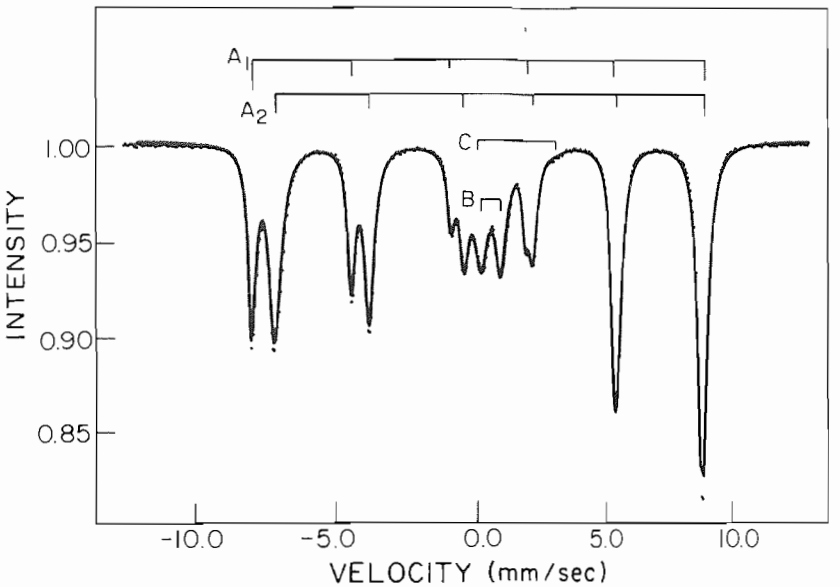

Figure 9. Mössbauer spectrum of *A. magnetotacticum* wet packed cells at 200°K.

spectral characteristics B. Thawing and aeration of these frozen cells result in increases in B spectral lines and concomitant decreases in C spectral lines. This indicates that the iron atoms responsible for spectrum C came from reduction of the iron atoms giving spectrum B. Unlike that of spectrum B, the intensity of spectrum C does not decrease between 80 and 4.2°K.

The decrease in the intensity of spectrum B between 80 and 4.2°K can be explained as the onset of magnetic hyperfine interactions at low temperature resulting in a concomitant decrease in the intensity of the central absorption doublet. This phenomenon has been observed with Mössbauer spectroscopy of ferritin and hemosiderin (Fig. 6). However,

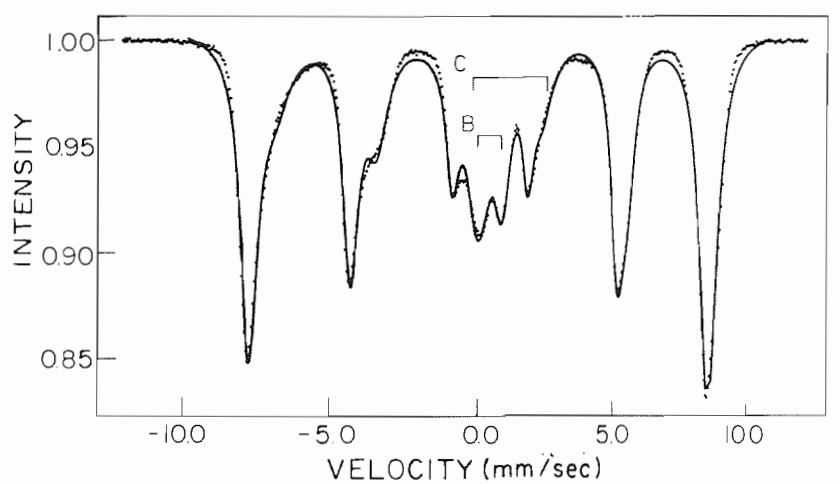

Figure 10. Mössbauer spectrum of *A. magnetotacticum* wet packed cells at 80°K.

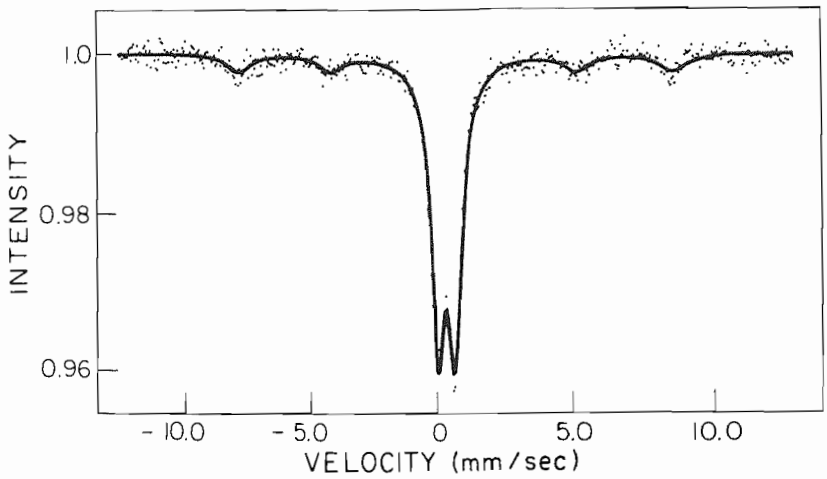

Figure 11. Mössbauer spectrum of nonmagnetotactic cells at 80°K. Some residual Fe_3O_4 is present in the sample.

in the present case, the magnetic hyperfine lines are obscured by the magnetite spectral lines (A_1 and A_2). To further resolve the nature of the material responsible for spectrum B, we studied the temperature-dependent Mössbauer spectra of nonmagnetotactic cells which lacked the interfering magnetite.

For $T \geq 80$°K, the spectrum of lyophilized nonmagnetotactic cells (Fig. 11) consists primarily of the quadrupole doublet characteristic of ferric iron as denoted by spectrum B in Figs. 9 and 10. In addition, a very-low-intensity spectrum due to Fe_3O_4 (spectral lines $A_1 + A_2$ in Fig. 9) is observed. These latter spectral lines might be due to a small fraction of magnetotactic cells in the sample or trace amounts of magnetite possibly present in the nonmagnetotactic cells. Below 80°K, the intensity of the quadrupole doublet decreased with decreasing temperature while the intensity of a six-line spectrum flanking the doublet increased. At 4.2°K, the spectrum (Fig. 12) consists primarily of the six broadened magnetic hyperfine lines, with a small residual doublet in the center. The Fe_3O_4 spectrum was then obscured by the six-line spectrum. Application of a longitudinal magnetic field of 60 kOe produced broadening of the six-line spectrum but with no appreciable shifts in the line positions and no decreases in any line intensities.

These spectral characteristics are indicative of small particles of hydrous ferric oxide with antiferromagnetic exchange interactions similar to those of the ferrihydrite within ferritin micelles. If we use values of K and f_0 appropriate to ferritin, the experimental results indicate that hydrous ferric oxide particles in the nonmagnetotactic cells are of the order of 100 Å in diameter, or less. Unlike ferritin or ferrihydrite, however, there is a residual quadrupole doublet in the 4.2°K spectra of magnetotactic and nonmagnetotactic cells. The intensity of this residual doublet varies somewhat from sample to sample, but its presence suggests another high-spin ferric iron material with high-temperature spectral characteristics similar to those of ferrihydrite, but with iron atoms less densely packed so that magnetic exchange interactions between them are weaker and the spectrum is not magnetically split at 4.2°K. This latter material is more easily studied in a cloned, nonmagnetotactic strain of *A. magnetotacticum* that accumulates less iron.

The Mössbauer spectrum of wet packed cells of the cloned, nonmagnetotactic strain consists of a quadrupole absorption doublet for $T \gtrsim 4.2$°K (Fig. 13). The spectral parameters obtained at 80°K were similar to those of spectrum B in magnetotactic cells (Table I),

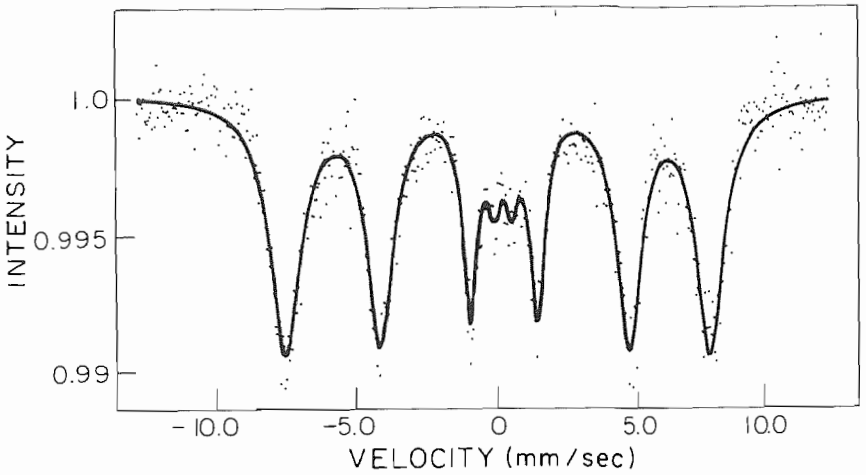

Figure 12. Mössbauer spectrum of nonmagnetotactic cells at 4.2°K.

indicating the presence of a high-spin ferric iron material. Application of an external 60-kOe magnetic field at 4.2°K results in spectra with a broad distribution of hyperfine fields. These spectral characteristics indicate the presence of high-spin Fe^{3+} in a hydrous oxide with magnetic exchange interactions of the order of 2–3°K, that is, where the iron atoms are less densely packed than in ferrihydrite. This material has similar spectral characteristics to the iron storage material in *E. coli* (Bauminger *et al.*, 1980).

When the wet packed cells were held above 275°K in an anaerobic environment, a ferrous spectrum similar to spectrum C appeared, in addition to the ferric iron doublet. This indicates that the hydrous ferric oxide in cells of this strain can be reduced to ferrous iron as with cells of the other strains.

Diffusive motions of the magnetosomes in *A. magnetotacticum* have been observed in the Mössbauer spectrum of whole cells above 275°K. The temperature dependence of

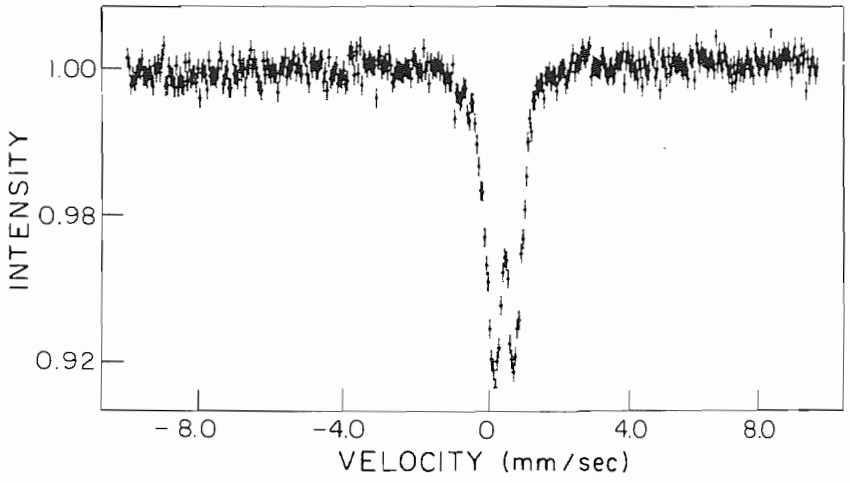

Figure 13. Mössbauer spectrum of cloned, nonmagnetotactic strain of *A. magnetotacticum* at 4.2°K.

the ferrihydrite spectrum is consistent with the association of the ferrihydrite with the magnetosomes. Ferrous iron in the cells appears to be associated with the peptidoglycan of the cell wall (Ofer *et al.*, 1984).

The foregoing results suggest that *A. magnetotacticum* precipitates Fe_3O_4 in the sequence (1) Fe^{3+} quinate → (2) low-density hydrous ferric oxide → (3) high-density hydrous ferric oxide (ferrihydrite) → (4) Fe_3O_4 with Fe^{2+} appearing as a transient between (1) and (2). Because ferrihydrite contains ferric iron only, (3) → (4) implies reduction of one-third of the iron atoms. The deposition of ferrihydrite and subsequent reductions and precipitation of Fe_3O_4 occur in the magnetosome envelope. High resolution transmission electron microscopy gives evidence for an amorphous (ferrihydrite) phase as well as single crystal Fe_3O_4 with well defined morphology and orientation in the magnetosomes (Mann *et al.*, 1984).

Reduction of a ferrihydrite precursor to Fe_3O_4 occurs in the marine chiton, a mollusc of the order Polyplacophora. In this organism, the radular teeth undergo a sequential mineralization process that results in a surface coating of Fe_3O_4. Iron is transported to the superior epithelial cells of the radula in the storage protein ferritin. Then, iron is transferred to a preformed organic matrix on the tooth surface as ferrihydrite. Finally, the ferrihydrite is reduced to Fe_3O_4. The resulting Fe_3O_4 particles have dimensions of the order of 0.1 μm (Towe and Lowenstam, 1967; Kirschvink and Lowenstam, 1979).

Cells containing hydrous iron oxide granules have been found in the bands around each abdominal segment in honeybees (Kuterbach *et al.*, 1982). Honeybees are sensitive to the geomagnetic field and are known to have Fe_3O_4 in their abdomens (Gould *et al.*, 1978). Some of the hydrous iron oxide in the granules could serve as a precursor to Fe_3O_4 formation.

Thus, Fe_3O_4 precipitation might follow similar pathways in a wide variety of organisms. In the bacteria, however, we have the best opportunity to elucidate the biochemical details of the process and its connection to overall cellular metabolism.

ACKNOWLEDGMENTS. R.B.F. and G.C.P. were partially supported by the Office of Naval Research. The Francis Bitter National Magnet Laboratory is supported by the National Science Foundation. R.P.B. was supported by the Office of Naval Research and the National Science Foundation.

References

Armstrong, R. J., Morrish, A. H., and Sawatzky, G. A., 1966, Mössbauer study of ferric ions in the tetrahedral and octahedral sites of a spinel, *Phys. Lett.* **23**:414–416.

Balkwill, D. L., Maratea, D., and Blakemore, R. P., 1980, Ultrastructure of a magnetotactic spirillum, *J. Bacteriol.* **141**:1399–1408.

Bancroft, G. M., 1973, *Mössbauer Spectroscopy: An Introduction for Inorganic Chemists and Geochemists*, McGraw-Hill, New York.

Banerjee, S. K., O'Reilly, W., and Johnson, C. E., 1967, Mössbauer effect measurements in FeTi spinels with local disorder, *J. Appl. Phys.* **38**:1289–1291.

Bauminger, E. R., Cohen, S. G., Dickson, D. P. E., Levy, A., Ofer, S., and Yariv, J., 1980, Mössbauer spectroscopy of *E. coli* and its iron storage protein, *Biochim. Biophys. Acta* **623**:237–242.

Blaise, A., Chappert, J., and Givadet, J. L., 1965, Observation par mesures magnétiques et effet Mössbauer d'un antiferromagnétisme de grains fins dans la ferritine, *C. R. Acad. Sci.* **261**:2310–2313.

Blakemore, R. P., 1975, Magnetotactic bacteria, *Science* **190**:377–379.

Blakemore, R. P., 1982, Magnetotactic bacteria, *Annu. Rev. Microbiol.* **36**:217–238.

Blakemore, R. P., and Frankel, R. B., 1981, Magnetic navigation in bacteria, *Sci. Am.* **245**(6):58–65.

Blakemore, R. P., Maratea, D., and Wolfe, R. S., 1979, Isolation and pure culture of a freshwater magnetic spirillum in chemically defined medium, *J. Bacteriol.* **140**:720–729.

Blakemore, R. P., Frankel, R. B., and Kalmijn, A. J., 1981, South-seeking magnetotactic bacteria in the southern hemisphere, *Nature* **286**:384–385.

Chappert, J., Teillet, J., and Varret, F., 1979, Recent developments in high field Mössbauer spectroscopy, *J. Magn. Magn. Mater.* **11**:200–207.

Coey, J. M. D., and Readman, P. W., 1973, Characterization and magnetic properties of a natural ferric gel, *Earth Planet. Sci. Lett.* **21**:45–51.

Cohen, R. L. (ed.), 1976, *Applications of Mössbauer Spectroscopy*, Volume I, Academic Press, New York.

Cohen, R. L. (ed.), 1981, *Applications of Mössbauer Spectroscopy*, Volume II, Academic Press, New York.

Dezsi, I., Keszthelyi, L., Kulgawczuk, D., Molnár, B., and Eissa, N. A., 1967, Mössbauer study of β and δ-FeOOH, *Phys. Status Solidi* **22**:617–629.

Forsyth, J. B., Hedley, I. G., and Johnson, C. E., 1968, The magnetic structure and hyperfine field of goethite (δ-FeOOH), *J. Phys. C (Ser. 2)* **2**:179–188.

Frankel, R. B., 1982, Magnetotactic bacteria, *Comments Mol. Cell. Biophys.* **1**:293–310.

Frankel, R. B., and Blakemore, R. P., 1980, Navigational compass in magnetic bacteria, *J. Magn. Magn. Mater.* **15–18**:1562–1564.

Frankel, R. B., Blakemore, R. P., and Wolfe, R. S., 1979, Magnetite in freshwater magnetotactic bacteria, *Science* **203**:1355–1356.

Frankel, R. B., Blakemore, R. P., Torres de Araujo, F. F., Esquivel, D. M. S., and Danon, J., 1981, Magnetotactic bacteria at the geomagnetic equator, *Science* **212**:1269–1270.

Frankel, R. B., Papaefthymiou, G. C., Blakemore, R. P., and O'Brien, W. D., 1983, Fe_3O_4 precipitation in magnetotactic bacteria, *Biochim. Biophys. Acta* **763**:147–159.

Freeman, A. J., and Frankel, R. B., 1967, *Hyperfine Interactions*, Academic Press, New York.

Gould, J. L., Krischvink, J. L., and Deffeyes, K. S., 1978, Bees have magnetic remanence, *Science* **201**:1026–1028.

Greenwood, N. N., and Gibb, T. C., 1971, *Mössbauer Spectroscopy*, Chapman & Hall, London.

Hargrove, R. S., and Kundig, W., 1970, Mössbauer measurements of magnetite below the Verwey transition, *Solid State Commun.* **8**:303–308.

Johnson, C. E., 1969, Antiferromagnetism of γ-FeOOH: A Mössbauer effect study, *J. Phys. C (Ser. 2)* **2**:1996–2002.

Kaufman, K. S., Papaefthymiou, G. C., Frankel, R. B., and Rosenthal, A., 1980, Nature of iron deposits on the cardiac walls in β-thalassemia by Mössbauer spectroscopy, Biochim. Biophys. Acta **629**:522–529.

Kirschvink, J. L., 1980, South-seeking magnetic bacteria, *J. Exp. Biol.* **86**:345–347.

Kirschvink, J. L., and Lowenstam, H. A., 1979, Mineralization and magnetization of chiton teeth: Paleomagnetic, sedimentologic and biologic implications of organic magnetite, *Earth Planet. Sci. Lett.* **44**:193–204.

Kuterbach, D. A., Walcott, B., Reeder, R. J., and Frankel, R. B., 1982, Iron-containing cells in the honeybee (*Apis mellifera*), *Science* **218**:695–697.

Lowenstam, H. A., and Rossman, G. R., 1975, Amorphous, hydrous, ferric phosphatic dermal granules in *Molpadia* (Holothuroidea): Physical and chemical characterization and ecological implications of the bioinorganic fraction, *Chem. Geol.* **15**:15–51.

Mann, S., Frankel, R. B., and Blakemore, R. P., 1984, Structure, morphology and crystal growth of bacterial magnetite, *Nature* **310**:405–407.

McNabb, T. K., Fox, R. A., and Boyle, A. J. F., 1968, Some magnetic properties of magnetite (Fe_3O_4) microcrystals, *J. Appl. Phys.* **39**:5703–5711.

Moench, T. T., and Konetzka, W. A., 1978, A novel method for the isolation and study of magnetotactic bacterium, *Arch. Microbiol.* **119**:203–212.

Murad, E., and Schwertmann, U., 1980, The Mössbauer spectrum of ferrihydrite and its relations to those of other iron oxides, *Am. Mineral.* 65:1044–1049.

Ofer, S., Nowik, I., Bauminger, E. R., Papaefthymiou, G. C., Frankel, R. B., and Blakemore, R. P., 1984, Magnetosome dynamics in magnetotactic bacteria, *Biophys. J.* **46**:57–64.

Ofer, S., Papaefthymiou, G. C., Frankel, R. B., and Lowenstam, H. A., 1981, Mössbauer spectroscopy of iron-containing dermal granules from *Molpadia intermedia*, *Biochim. Biophys. Acta* **676**:199–204.

Oosterhuis, W. T., and Spartalian, K., 1976, Biological iron transport and storage compounds, in: *Applications of Mössbauer Spectroscopy*, Volume I (R. L. Cohen, ed.), Academic Press, New York, pp. 141–170.

Towe, K. M., and Moench, T. T., 1981, Electron-optical characterization of bacterial magnetite, *Earth Planet. Sci. Lett.* **52**:213–220.

van der Woude, F., 1966, Mössbauer effect in α-Fe_2O_3, *Phys. Status Solid.* **17**:417–432.